Korean J. Chem. Eng., **26**(6), 1441-1446 (2009)
DOI: 10.1007/s11814-009-0230-7

Thermal instability of a fluid layer when cooled isothermally from above

Joo Hyung Moon*, Kyung Hyun Ahn*,†, Chang Kyun Choi*, and Min Chan Kim**

*School of Chemical and Biological Engineering, Seoul National University, Seoul 151-744, Korea
**Department of Chemical Engineering, Jeju National University, Jeju 690-756, Korea
(*Received 8 February 2009 • accepted 15 March 2009*)

Abstract−The onset of buoyancy-driven convection in an initially motionless isothermal fluid layer is analyzed numerically. The infinite horizontal fluid layer is suddenly cooled from above to relatively low temperature. The rigid lower boundary remains at the initial temperature. In the present transient system, when the Rayleigh number Ra exceeds 1101, thermal convection sets in due to buoyancy force. To trace the temporal growth rates of the mean temperature and its fluctuations we solve the Boussinesq equation by using the finite volume method. We suggest that the system begins to be unstable when the growth rate of temperature disturbances becomes equal to that of the conduction field. Three different characteristic times are classified to interpret numerical results clearly: the onset time of intrinsic instability, the detection time of manifest convection and the undershoot time in a plot of the cooling rate versus time. The present scenario is that the thermal instability sets in at the critical time, then grows super-exponentially up to near the undershoot time, and between these two times the first visible motion is detected. Numerical results are compared with available experimental data. It is found that the above scenario looks promising and the critical time increases with decreasing the Prandtl number Pr and also the Rayleigh number Ra.

Key words: Buoyancy-driven Convection, Growth Rate, Thermal Instability, Rayleigh Number

INTRODUCTION

When an initially motionless, horizontal fluid layer is either heated from below or cooled from above, convective motion can appear at a certain time by buoyancy forces. This is an example of evolving Rayleigh-Bénard convection. In this transient system, it is important to predict the critical time at which the convective instability would set in. Related instability studies have been carried out by using various methods such as the frozen-time model [1], propagation theory [2,3], amplification theory [4], stochastic model [5], and maximum-Rayleigh number criterion [6]. However, ambiguity still exists among characteristic times obtained from each model. The first two models are based on linear theory and yield the characteristic times which exhibit the fastest growing mode of instabilities. The others deal with the onset time of manifest convection. But it is known that the thermal convection can be detected before the manifestation of convection. The first and the last model cannot demonstrate the effect of the Prandtl number. The third and the fourth require initial conditions and criterion to define manifest convection.

A free boundary system is encountered in evaporation and separation processes. Spangenberg and Rowland [7] and Foster [8] conducted experiments with water under evaporative cooling. In gas absorption systems, Plevan and Quinn [9], Blair and Quinn [10], Mahler and Schechter [11], and Tan and Thorpe [12] conducted experiments to measure the onset times of buoyancy-driven convection.

In the present study the onset of thermal instability in a horizontal fluid layer cooled isothermally from above is analyzed numerically. Dependence of characteristic times on Pr and Ra is also investigated. To represent the transient behavior of convective instability, three different characteristic times are classified for high Ra. The critical time to mark the onset time of intrinsic instability, t_c, is defined. At this time its magnitude is not large enough to be detected. Therefore, some growth period would be required until manifest motion is surely observed at $t=t_D$. In a plot of the cooling rate versus time, the minimum is exhibited at $t=t_u$. Here the difference among the above characteristic times will be clarified numerically. We will trace the behavior of convective instability with time and compare the resulting characteristic times with available experimental data.

GOVERNING EQUATIONS

The system considered here is a horizontal fluid layer under free-rigid boundary subject to isothermal cooling from above. A schematic diagram of the system is shown in Fig. 1. The horizontal fluid layer of thickness H with homogeneous initial temperature T_i is cooled rapidly from above at $t\geq 0$. The free upper boundary is kept at constant lower temperature T_u, whereas the rigid lower boundary remains still at the initial one T_i. In a suddenly cooled system nonlinear time-dependent temperature profile is developed and buoyancy-driven

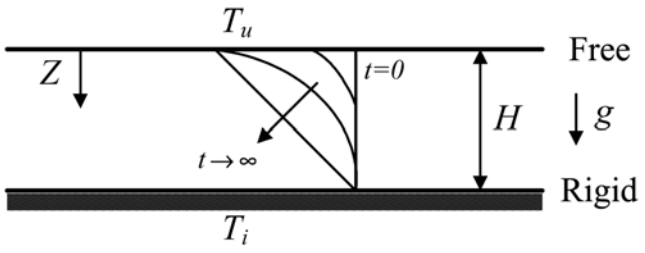

Fig. 1. Schematic diagram of the present system.

†To whom correspondence should be addressed.
E-mail: ahnnet@snu.ac.kr

convection will set in at a certain time before a final linear temperature profile is formed. The governing equations of flow and temperature fields in the convection regime are expressed in dimensionless form by employing the Boussinessq approximation as follows:

$$\nabla \cdot \mathbf{u} = 0, \tag{1}$$

$$\left\{\frac{\partial}{\partial \tau} + \mathbf{u}\cdot\nabla\right\}\mathbf{u} = -\nabla p + Pr\nabla^2\mathbf{u} + PrRa\theta\mathbf{k}, \tag{2}$$

$$\left\{\frac{\partial}{\partial \tau} + \mathbf{u}\cdot\nabla\right\}\theta = \nabla^2\theta, \tag{3}$$

with the boundary conditions,

$$\frac{\partial u}{\partial z} = \frac{\partial v}{\partial z} = w = \frac{\partial^2 w}{\partial z^2} = 0, \quad \theta = 1 \text{ at } z = 0, \tag{4a, b}$$

$$u = v = w = \frac{\partial w}{\partial z} = 0, \quad \theta = 0 \text{ at } z = 1, \tag{5a, b}$$

where z, θ, p, τ, and **u** denote the dimensionless forms of the vertical length Z, the temperature excess $T_i - T$, the dynamic pressure P, the time t, and the velocity vector **U**. The latter ones have been nondimensionalized by using H, $\Delta T(=T_i - T_u)$, $H^2/(\rho\alpha^2)$, α/H^2 and H/α, respectively. Here α, g, ρ, and **k**, respectively, represent the thermal diffusivity, the gravitational acceleration constant, the fluid density at $T=T_i$, and the vertical unit vector. The important parameters to characterize the onset of convective motion in the system are the Rayleigh number Ra, and the Prandtl number Pr:

$$Ra = \frac{g\beta\Delta T H^3}{\alpha\nu}, \quad Pr = \frac{\nu}{\alpha}, \tag{6a, b}$$

where β is the thermal expansion coefficient and ν is the kinematic viscosity.

THEORETICAL ANALYSES

The velocity and temperature fields can be decomposed into the horizontal mean values and their fluctuations as follows:

$$\mathbf{u} = \langle \mathbf{u} \rangle + \mathbf{u}', \tag{7}$$

$$\theta = \langle \theta \rangle + \theta', \tag{8}$$

where <·> and ′ represent the mean quantities and their fluctuations, respectively. The mean quantity is a function of τ and z, and it is known that <**u**>=0 for the flow in form of regular even cells. Based on the experimental observations, fluctuations are assumed to be periodic as follows:

$$[\theta', \mathbf{u}'] \cong [A(\tau)\theta^*(z), B(\tau)\mathbf{u}^*(z)]\exp[i(a_x x + a_y y)] \text{ for } 0 \le \tau \le \tau_c, \tag{9}$$

where A and B are the magnitudes of fluctuations, i is the imaginary number, a_x and a_y are the dimensionless wavenumbers in the x- and the y- direction, respectively, and τ_c represents the critical time to mark the onset of intrinsic instability. The functions θ^* and $\mathbf{u}^*$ denote the normalized temperature and velocity fluctuations, respectively.

For an infinite horizontal layer shown in Fig. 1, only y may be used as the horizontal distance with $a=a_y$, where $a(=\sqrt{a_x^2 + a_y^2})$ is the dimensionless horizontal wavenumber. The initial conditions at $\tau=0$ are constructed as follows:

$$\theta' = A(0)\theta^*(z)\cos(ay), \tag{10a}$$

$$v' = -B(0)((\partial w^*(z)/\partial z)/a)\sin(ay), \tag{10b}$$

$$w' = B(0)w^*(z)\cos(ay), \tag{10c}$$

where v′ and w′ are the horizontal and the vertical velocity fluctuations, respectively. Here A(0) and B(0) are the initial magnitudes of the fluctuations. It is assumed that θ^* and $\mathbf{u}^*$ would not change for $0 \le \tau \le \tau_c$. This implies that the unique disturbance patterns are determined with the converged disturbance profiles obtained by iterative calculation for $0 \le \tau \le \tau_c$.

In the present system thermal convection sets in due to the buoyancy force and its magnitude F_B is given by

$$F_B = \rho g \beta |T - T_i|, \tag{11}$$

which is produced by temperature differences. The buoyancy force can also be divided into two terms based on the mean temperature and its fluctuations. They are expressed as $(F_{B,0}, F_{B,1}) = (<\theta>, \theta')\rho g\beta\Delta T$, respectively. To examine the transient behaviors of thermal instabilities, the following temporal growth rates are defined here:

$$r_{0,T} = \frac{1}{\langle\theta\rangle_{rms}}\frac{d\langle\theta\rangle_{rms}}{d\tau}, \tag{12}$$

$$r_{1,T} = \frac{1}{\theta'_{rms}}\frac{d\theta'_{rms}}{d\tau}, \tag{13}$$

where $r_{0,T}$ and $r_{1,T}$ are the temporal growth rates of the mean temperature and its temperature fluctuations, respectively. Here the subscript rms refers to the root-mean-square quantity, i.e., $(\cdot)_{rms} = [\int_V (\cdot)^2 dV/V]^{1/2}$, where V represents the volume of the system considered. In the same manner, the temporal growth rate of velocity fluctuations is defined as follows:

$$r_{1,V} = \frac{1}{\mathbf{u}'_{rms}}\frac{d\mathbf{u}'_{rms}}{d\tau}, \tag{14}$$

where $\mathbf{u}'_{rms} = [\int_V |\mathbf{u}|^2 dV/V]^{1/2}$.

Along with above three growth rates, the critical condition of intrinsic instability is suggested here [13-16]:

$$r_{1,T} = r_{0,T} \text{ with } r_{1,V} \ge 0 \text{ at } \tau = \tau_c. \tag{15}$$

This means that the characteristic motion of $a=a_c$ to satisfy Eq. (9) sets in at the earliest time τ_c. For $\tau < \tau_c$, fluctuations are quite small in comparison with the mean temperature field controlled by conduction and they may be regarded as noises. For $\tau > \tau_c$, buoyancy-driven instabilities grow with time and they are detected at a certain time. Therefore, the system is assumed to be stable when $r_{1,T} < r_{0,T}$ but unstable when $r_{1,T} > r_{0,T}$.

In the present study the Nusselt number Nu with the characteristic length of H is defined as follows:

$$Nu = \int_S (-\partial\theta/\partial z)_{z=0} dS/S, \tag{16}$$

where S is the surface area of the upper plate with $\theta=1$ at z=0. When convection sets in, Nu starts to deviate from its conduction solution

and has a minimum at $\tau=\tau_u$. The undershoot time τ_u is frequently used as the characteristic time to represent the manifest convection.

NUMERICAL METHODS

We solved governing Eqs. (1)-(3) numerically by using the finite volume method (FVM) [17]. Two-dimensional motion with horizontal periodicity was considered. Accordingly, one convection cell with the proper side-boundary conditions was chosen to describe the horizontal infinite layer. The SIMPLE algorithm was applied to solve the pressure equation connected with the continuity equation, and the hybrid scheme was used to formulate the discretization equations. To solve the present time-dependent problem, the implicit method was adopted and the first-order time increment was used. The number of meshes was 42×60 and finer meshes were used near the top and bottom boundaries to guarantee the physical validity. Also, to ensure the numerical stability the time step of $\Delta\tau=10^{-7}$ was used. In the present time-dependent problem, the convergence was assumed when the changes of velocities and temperature were smaller than 10^{-6} at each time step.

With the proper magnitude of the initial temperature and velocity amplitudes A(0) and B(0), the present system was simulated numerically for a given Ra and Pr. The proper A(0)-values were chosen in the range of $10^{-4}\le A(0)\le 10^{-2}$ after comparing with the experimental data. In the present study, numerical simulation was conducted for Pr≥0.7 and $10^5\le Ra\le 10^8$, and the τ_c- and τ_u-values were obtained numerically.

RESULTS AND DISCUSSION

The results of the numerical simulation by the FVM with various Pr and Ra are reported here. Based on Eqs. (12)-(14), the stability criterion to satisfy the condition (15) is used to represent a fastest growing mode of instability. This concept has been developed by Choi et al. [14] and Park et al. [15]. Especially, Park et al. [16] analyzed the present system for Pr→∞ and $Ra=10^6$. Here we extend their work for the cases of Pr≥0.7 and $10^5\le Ra\le 10^8$.

With Pr=7, $Ra=10^6$ and $A(0)=10^{-3}$, the temporal behaviors of fluctuations are shown in Fig. 2. For small τ, w'_{rms} and θ'_{rms} keep almost the same magnitudes as their initial ones. But right after the critical time τ_c, they experience a sudden increase. The temporal growth rates given by Eqs. (12)-(14) are depicted in Fig. 3. The stability criterion (15) yields $\tau_c=2.383\times10^{-4}$ and $a_c=15$ for $Ra=10^6$ and Pr=7. The maximum values of $r_{1,T}$ and $r_{1,V}$ appear at $\tau=\tau_{m,T}$ and $\tau=\tau_{m,V}$, respectively. It is noted that they are almost the same for each A(0)-value. This figure also shows that the τ_c-value is independent of the A(0)-value for $10^{-4}\le A(0)\le 10^{-2}$ but the $\tau_{m,T}$- and

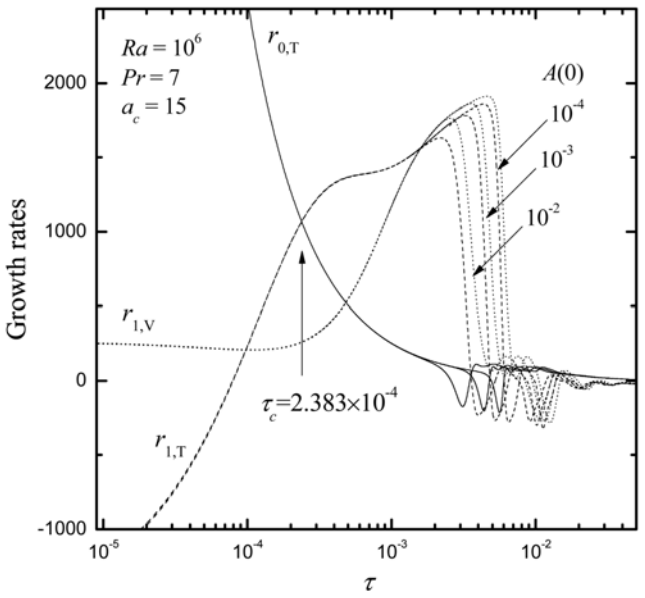

Fig. 3. Temporal growth rates for Pr=7 and $Ra=10^6$ and their dependence upon A(0)-values.

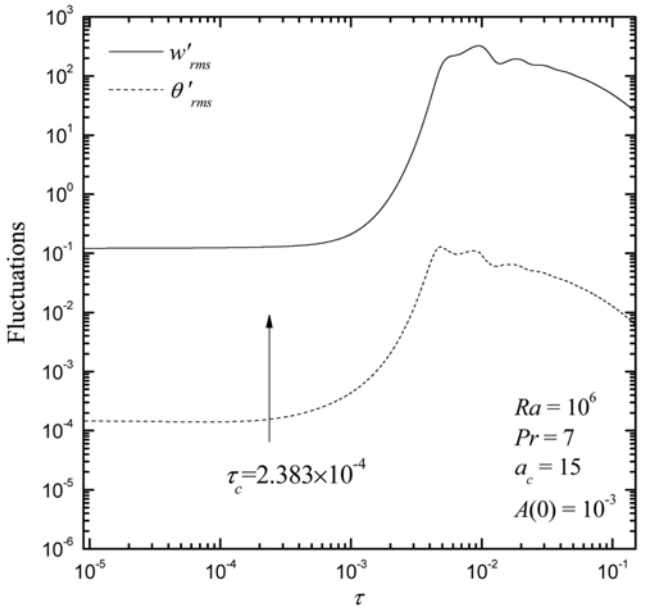

Fig. 2. Transient behaviors of fluctuations for Pr=7 and $Ra=10^6$.

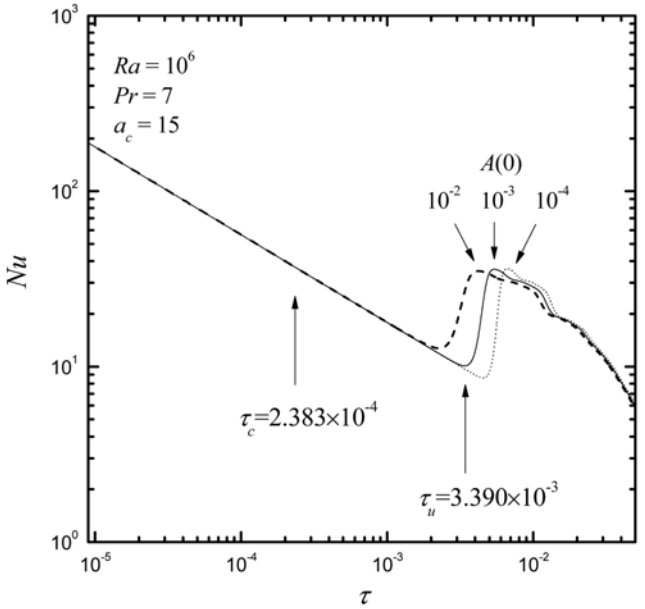

Fig. 4. Temporal Nusselt number for Pr=7 and $Ra=10^6$.

$\tau_{m,V}$-values are dependent upon it. Therefore, it is stated that the present τ_c-value is the invariant and it represents the onset time of intrinsic instability.

The developing behavior of the Nusselt number with time is illustrated in Fig. 4. The present numerical simulation yields the undershoot time τ_u=3.390×10^{-3} with A(0)=10^{-3} in a plot of Nu versus τ. The undershoot time represents the characteristic time of manifest convection. The τ_u-value is dependent upon the A(0)-value, as shown in the figure. Also, it is known that $\tau_u \cong \tau_{m,T} \cong \tau_{m,V}$. The incipient instability at $\tau=\tau_c$ will grow with increasing τ and convective motion will be detected at $\tau=\tau_D$. The detection time of motion is prior to the undershoot time of the Nusselt number. The detection time of convective motion may be closely connected with $r_{1,V}$ and the earliest detection time τ_D would be located between τ_c and $\tau_{m,V}$. Here the relation of $\tau_c \le \tau_D \le \tau_{m,V} (\cong \tau_u)$ is suggested.

Figs. 5 and 6 show temporal behaviors of growth rates and Nu along with Pr=0.7, 7, 100 and Pr→∞ for Ra=10^6 and A(0)=10^{-3}. As Pr decreases, the critical time and the undershoot time increase, whereas the maximum amplitude of growth rates of fluctuations decreases. As Ra decreases, similar behaviors are observed in Figs. 7 and 8. Therefore, it can be stated that lowering Pr and also Ra makes the system more stable.

Numerical results of the critical time τ_c and the corresponding wavenumber a_c obtained in this study are summarized in Table 1.

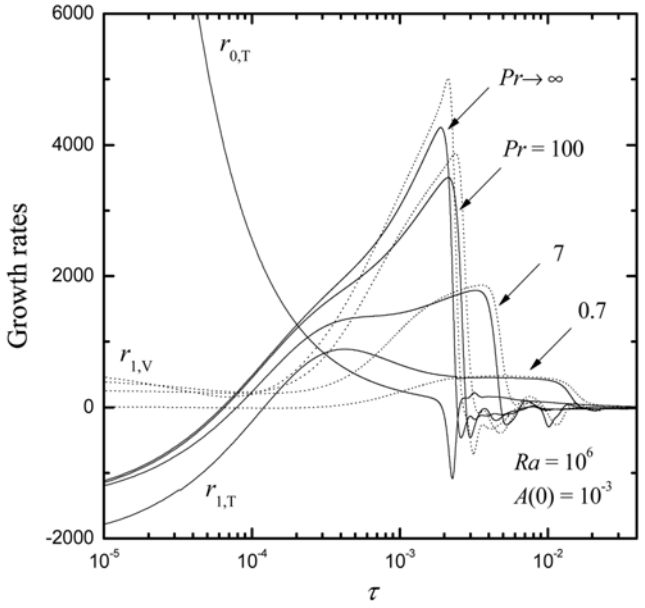

Fig. 5. Effect of Pr on temporal growth rates for Ra=10^6.

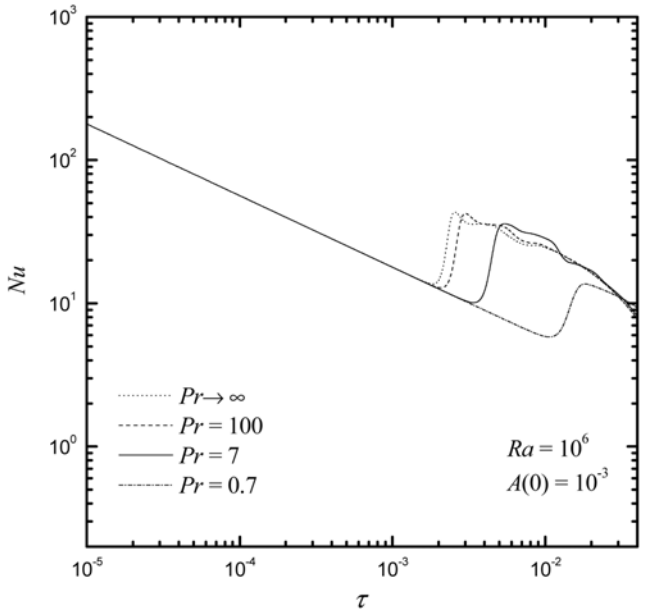

Fig. 6. Effect of Pr on Nu for Ra=10^6.

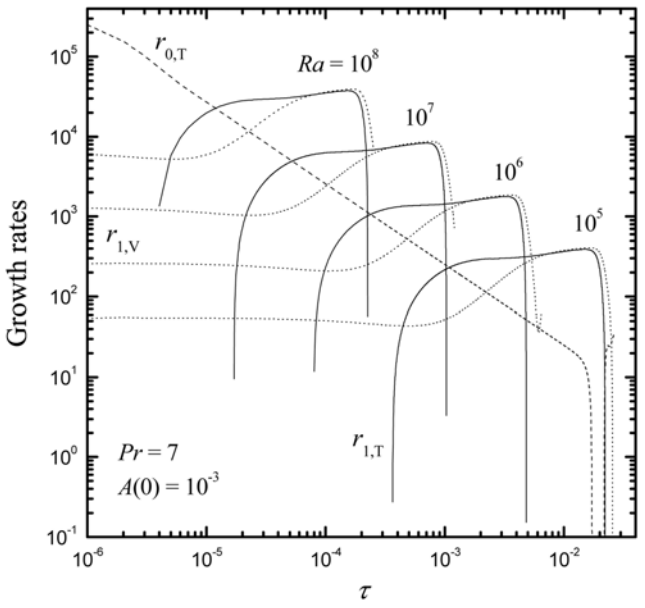

Fig. 7. Effect of Ra on temporal growth rates for Pr=7.

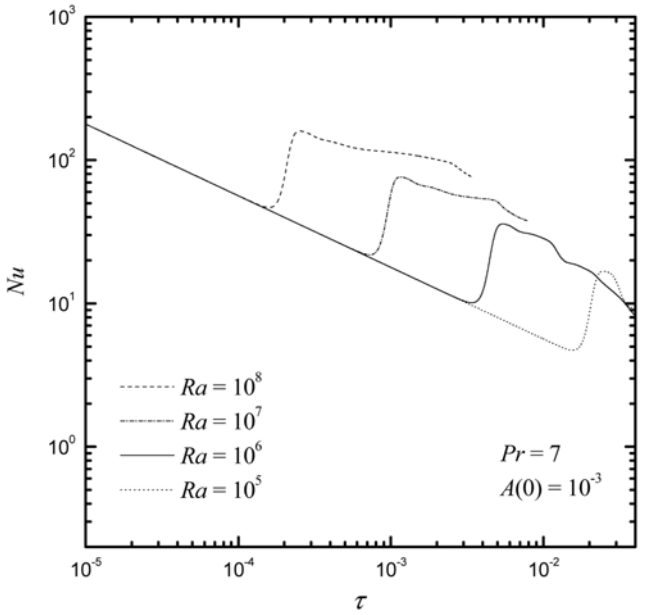

Fig. 8. Effect of Ra on Nu for Pr=7.

Table 1. Wavenumbers and critical times for various Pr and Ra

Ra	Pr→∞		Pr=100		Pr=7		Pr=0.7	
	a_c	$\tau_c\times10^4$	a_c	$\tau_c\times10^4$	a_c	$\tau_c\times10^4$	a_c	$\tau_c\times10^4$
10^5	5.5	9.188	5.6	9.471	7.0	10.91	12	14.12
10^6	11	2.020	12	2.069	15	2.383	27	3.079
10^7	24	0.4335	25	0.4485	32	0.5219	57	0.6919
10^8	52	0.09820	54	0.1009	70	0.1170	117	0.1579

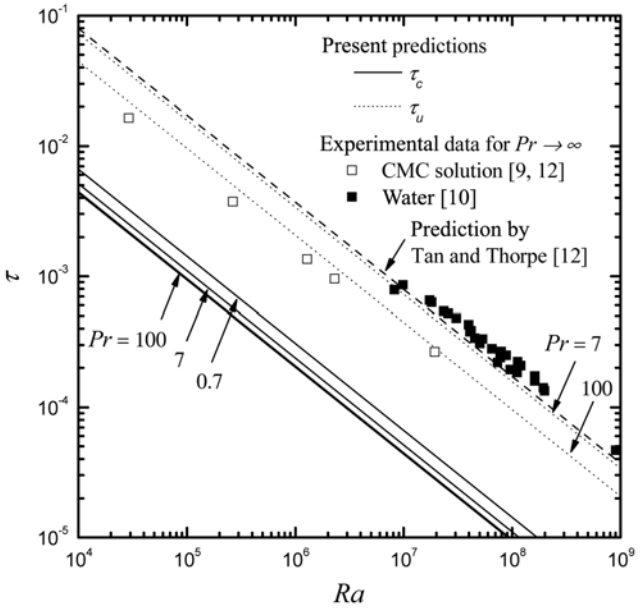

Fig. 9. Comparison with experimental data.

Based on these data, the following correlations of τ_c and a_c are found for Pr≥0.7 and $10^5\le Ra\le10^8$ within error bounds of 5.6% and 4.0%, respectively:

$$\tau_c = 2.63\left(0.375+\left(\frac{1.74}{Pr}\right)^{0.750}\right)^{0.237} Ra^{-2/3}, \quad (17)$$

$$a_c = 0.154\left(0.573+\left(\frac{1.83}{Pr}\right)^{0.772}\right)^{0.535} Ra^{1/3} \quad (18)$$

In Fig. 9 the present predictions are compared with experimental data. Plevan and Quinn [9] and Tan and Thorpe [12] investigated the onset time of convection in the case of gas absorption into aqueous carboxyl methyl cellulose (CMC) solutions. Blair and Quinn [10] also adopted the same gas absorption system except that they used water rather than CMC. Even though all these experimental data correspond to Pr→∞, comparison with them may provide a good measure to check the present predictions quantitatively. This is because the values for Pr=100 are not much different from those for Pr→∞ (see Table 1). As seen in Fig. 9, all experimental data deviate much from τ_c but are close to τ_u for Pr=7 or 100. This means that some growth period is required until convective motion becomes large enough to be detected experimentally. Therefore, τ_u is the time at which manifest convection is surely observed. Tan and Thorpe [12] provided correlations of τ_D similar to Eq. (17): $\tau_D=37.0\ Ra^{-2/3}$.

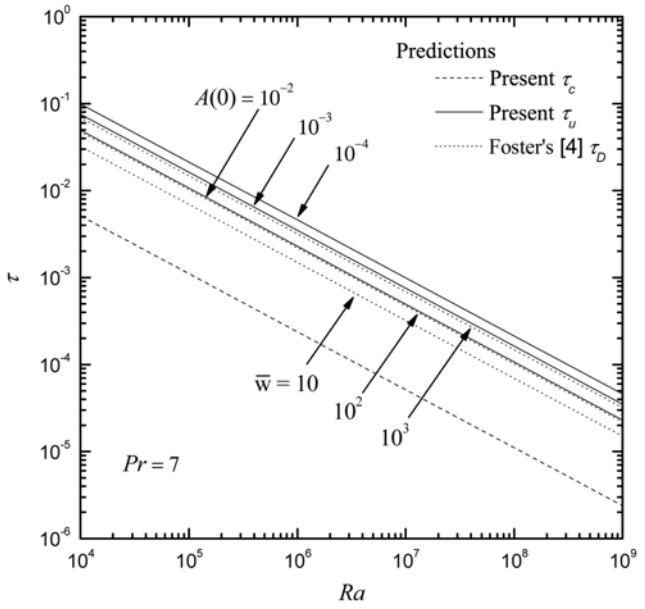

Fig. 10. Comparison with Foster's [4] predictions.

Their predicted times are larger than experimental ones for CMC solutions. Park et al. [16] reported that τ_u-values are very close to Blair and Quinn's [10] water data when they changed the free-rigid boundary conditions into the rigid-rigid ones for Pr→∞. This may be because a free upper surface behaves as if it is flexible but laterally rigid due to the presence of surface-active contaminants. However, this needs a further justification.

In the case of Pr=7 the present predictions are compared with those from Foster's [4] amplification theory in Fig. 10. Here $\overline{w}$ is the amplification factor. The present τ_c-values are smaller than his τ_D-ones. It is interesting that the present τ_u-values with $A(0)=10^{-2}$ and 10^{-3} are almost the same as Foster's τ_D-ones with $\overline{w}=10^2$ and $\overline{w}=10^3$, respectively.

CONCLUSIONS

When a horizontal fluid layer is cooled isothermally from above, the critical time to mark the onset of convective instability has been investigated by using the FVM along with various Prandtl and Rayleigh numbers. We suggest a unique criterion to determine the onset time of intrinsic instability: when $r_{1,T}=r_{0,T}$, the fastest growing mode of instability sets in. Since τ_c-values are independent of A(0) in the range of $10^{-4}\le A(0)\le10^{-2}$, τ_c is the invariant for a given Ra and Pr. Therefore, here it is called the onset time of *intrinsic* instability.

In the present study the characteristic times, τ_c and τ_u, have been predicted. The manifest convection is surely observed at $\tau=\tau_u$ and experimental data are located near the τ_u-values. The critical time τ_c is smaller than the undershoot time τ_u. This means that some growth period is required until the motion is detected. Since convective motion can be detected earlier than τ_u, we suggest the relation of $\tau_c\le\tau_D\le\tau_u$.

NOMENCLATURE

a : dimensionless wave number [-]

A(0) : amplitude of temperature fluctuation [-]
B(0) : amplitude of velocity fluctuation [-]
g : gravitational acceleration constant [m/s^2]
H : height of layer [m]
k : thermal conductivity [N/s·K]
Nu : Nusselt number [-]
P : pressure [N/m^2]
Pr : Prandtl number, ν/α [-]
$r_{0,T}$: growth rate of mean temperature [-]
$r_{1,T}$: growth rate of temperature fluctuation [-]
$r_{1,V}$: growth rate of velocity fluctuation [-]
Ra : Rayleigh number, $g\beta\Delta TH^3/(\alpha\nu)$ [-]
t : time [s]
T : temperature [K]
ΔT : excess temperature, $T_i - T$ [K]
u : dimensionless velocity vector, UH/α [-]
U : dimensional velocity vector [m/s]

Greek Letters

α : thermal diffusivity [m^2/s]
β : thermal expansion coefficient [1/K]
ν : kinematic viscosity [m^2/s]
θ : dimensionless temperature, $(T_i - T)/(T_i - T_u)$ [-]
ρ : density [kg/m^3]
τ : dimensionless time, $t\alpha/H^2$ [-]

Subscripts

c : critical state
i : initial state
rms : root-mean-square quantity
u : upper
0 : basic state
1 : perturbed state

REFERENCES

1. B. R. Morton, *Q. J. Mech. App. Math*., **10**, 433 (1957).
2. C. K. Choi, J. H. Park and M. C. Kim, *Heat Mass Trans*., **41**, 155 (2004).
3. C. K. Choi and K. H. Kang, *Phys. Fluids*, **9**, 7 (1997).
4. T. D. Foster, *Phys. Fluids*, **8**, 1249 (1965).
5. B. S. Jhaveri and G. M. Homsy, *J. Fluid Mech*., **114**, 251 (1982).
6. K. K. Tan and R. B. Thorpe, *Chem. Eng. Sci*., **51**, 4127 (1996).
7. W. G. Spangenberg and W. R. Rowland, *Phys. Fluids*, **4**, 743 (1961).
8. T. D. Foster, *Phys. Fluids*, **8**, 1770 (1965).
9. R. E. Plevan and J. A. Quinn, *AIChE J*., **12**, 894 (1965).
10. L. M. Blair and J. A. Quinn, *J. Fluid Mech*., **36**, 385 (1969).
11. E. G. Mahler and R. S. Schechter, *Chem. Eng. Sci*., **25**, 955 (1970).
12. K. K. Tan and R. B. Thorpe, *Chem. Eng. Sci*., **47**, 3565 (1992).
13. T. J. Chung, M. C. Kim and C. K. Choi, *Korean J. Chem. Eng*., **21**, 41 (2004).
14. C. K. Choi, J. H. Park, H. K. Park, H. J. Cho, T. J. Chung and M. C. Kim, *Int. J. Thermal Sci*., **43**, 817 (2004).
15. J. H. Park, T. J. Chung, C. K. Choi and M. C. Kim, *AIChE J*., **52**, 2677 (2006).
16. J. H. Park, M. C. Kim, J. H. Moon, S. H. Park and C. K. Choi, *IASME Transactions*, **2**, 1674 (2005).
17. S. V. Patankar, *Numerical heat transfer and fluid flow*, Taylor & Francis, New York (1980).